

In preparation for the Astrophysical Journal

## First Stellar Abundances in NGC 6822 from VLT-UVES and Keck-HIRES Spectroscopy <sup>1</sup>

K. A. Venn<sup>2</sup>

Macalester College, Saint Paul, MN, 55105 (venn@clare.physics.macalester.edu)

D. J. Lennon

Isaac Newton Group of Telescopes (ING), Santa Cruz de La Palma, Canary Islands, E-38780, Spain (djl@ing.iac.es)

A. Kaufer

European Southern Observatory, Alonso de Cordova 3107, Santiago, Chile (akaufer@eso.org)

J. K. McCarthy<sup>3</sup>

Palomar Observatory, California Institute of Technology, Pasadena, CA, 91125  
(jkmccarthy@pacbell.net)

N. Przybilla and R. P. Kudritzki<sup>4</sup>

Institut für Astronomie und Astrophysik, Universitäts-Sternwarte München, München, D-81679, Germany (nob@usm.uni-muenchen.de and kudritzki@usm.uni-muenchen.de)

M. Lemke<sup>5</sup>

Dr. Karl Remeis-Sternwarte, Bamberg, D-96049, Germany (ai26@sternwarte.uni-erlangen.de)

E.D. Skillman

Department of Astronomy, University of Minnesota, Minneapolis, MN, 55455  
(skillman@astro.umn.edu)

and

S. J. Smartt

Institute of Astronomy, University of Cambridge, Madingley Road, Cambridge, CB3 0HA  
(sjs@ast.cam.ac.uk)

---

<sup>1</sup>Based on observations obtained from the UVES commissioning at the Very Large Telescope (Kueyen), European Southern Observatory, Paranal, Chile, and the W.M. Keck Observatory, Hawaii. Keck is operated as a scientific partnership among the California Institute of Technology, the University of California, and the National Aeronautics and Space Administration, and was made possible by the generous financial support of the W. M. Keck Foundation.

## ABSTRACT

We have obtained the first high resolution spectra of individual stars in the dwarf irregular galaxy, NGC 6822. The spectra of the two A-type supergiants were obtained at the VLT and Keck Observatories, using UVES and HIRES, respectively. A detailed model atmospheres analysis has been used to determine their atmospheric parameters and elemental abundances. The mean iron abundance from these two stars is  $\langle[\text{Fe}/\text{H}]\rangle = -0.49 \pm 0.22 (\pm 0.21)^6$ , with Cr yielding a similar underabundance,  $\langle[\text{Cr}/\text{H}]\rangle = -0.50 \pm 0.20 (\pm 0.16)$ . This confirms that NGC 6822 has a metallicity that is slightly higher than that of the SMC, and is the first determination of the present-day iron-group abundances in NGC 6822. The mean stellar oxygen abundance,  $12+\log(\text{O}/\text{H})=8.36 \pm 0.19 (\pm 0.21)$ , is in good agreement with the nebular oxygen results. Oxygen has the same underabundance as iron,  $\langle[\text{O}/\text{Fe}]\rangle = +0.02 \pm 0.20 (\pm 0.21)$ . This O/Fe ratio is very similar to that seen in the Magellanic Clouds, which supports the picture that chemical evolution occurs more slowly in these lower mass galaxies, although the O/Fe ratio is also consistent with that observed in comparatively metal-poor stars in the Galactic disk. Combining all of the available abundance observations for NGC 6822 shows that there is no trend in abundance with galactocentric distance. However, a subset of the highest quality data are consistent with a radial abundance gradient. More high quality stellar and nebular observations are needed to confirm this intriguing possibility.

*Subject headings:* stars: abundances, atmospheres, supergiants — galaxies: abundances, individual (NGC6822), stellar content

## 1. Introduction

Understanding the evolution of chemical abundances in galaxies provides an important constraint for uniquely determining their star formation histories. This is because prior stellar

---

<sup>2</sup>Adjunct Assistant Professor, Department of Astronomy, University of Minnesota, Minneapolis, MN, 55455

<sup>3</sup>Present address: Pixel Vision, Inc., Advanced Imaging Sensors Division, 4952 Warner Avenue, Suite 300, Huntington Beach, CA, 92649. Also, Adjunct Assistant Professor of Physics, Loyola Marymount University, 7900 Loyola Blvd., Los Angeles, CA, 90045.

<sup>4</sup>Max Planck Institut für Astrophysik, Garching, D-85740, Germany

<sup>5</sup>Present Address: INA-Werk Schaeffler, Herzogenaurach, Germany

<sup>6</sup>In this paper, abundances shall be reported with two uncertainties; the first is the line-to-line scatter, and the second (in parentheses and italics) is an *estimate* of the systematic error due to uncertainties in the atmospheric parameters.

nucleosynthesis information is preserved in the metallicity distribution of both the stars and gas. The analysis of bright nebular emission lines of H II regions has been the most frequent approach to modelling chemical evolution of galaxies to date (c.f., Pagel 1997). And yet, only a very limited number of elements can be examined and quantified when using this approach. The chemical evolution of a galaxy depends on the contributions of all its ISM-enriching constituents (e.g., type I supernovae, high mass stars, thermal pulsing intermediate AGB stars). Thus, more elements than just those observed from nebular studies need to be measured, since each has a different formation site which sample different constituents (e.g., oxygen is created primarily in massive stars, while iron comes from supernovae of both high and low mass stars). The need for abundances of heavy elements, and the new opportunities made possible by the 8- to 10-m telescopes and efficient high resolution spectrographs, have motivated us to determine elemental abundances in young stars in nearby galaxies. In this paper, we present our first results from an analysis of two A-type supergiants in NGC 6822.

NGC 6822 is a well-studied Local Group dwarf irregular galaxy with a distance modulus of  $23.49 \pm 0.08$  (Gallart *et al.* 1996a). Its stellar content has been extensively examined (see Chapter 9 in van den Bergh 2000 for a recent review), and it is known to have a low metallicity from nebular analyses. Its oxygen abundance was found to be  $12+\log(\text{O}/\text{H})=8.25 \pm 0.07$  from a study of seven H II regions (Pagel *et al.* 1980, or  $8.14 \pm 0.08$  considering only those H II regions where O III  $\lambda 4363$  was detected). These results are also supported by oxygen abundances from planetary nebulae (Richer & McCall 1995, Dufour & Talent 1980). This result is slightly higher than in the SMC ( $12+\log(\text{O}/\text{H})=8.1$ ), as found from both nebular and stellar analyses (c.f., Garnett *et al.* 1995, Venn 1999 and references therein).

A metallicity intermediate between the SMC and the LMC has also been reported from indirect observational data, e.g., the colors and spectral type distributions of red supergiants (Elias & Frogel 1985) and the relative color of an S star (Aaronson *et al.* 1985). Also, the number of WR stars to the number of massive stars in NGC 6822, which appears to be related to the metallicity of the galaxy, is between the number ratios in the LMC and SMC (Armandroff & Massey 1985, Azzopardi *et al.* 1988). However, a study of OB stellar spectral types by Massey *et al.* (1995) suggested that NGC 6822 may have a somewhat lower metallicity than the SMC based on weak metal line strengths. This claim has been refuted by a recent low resolution study of blue supergiants using VLT FORS by Muschielok *et al.* (1999). Muschielok *et al.* also suggest a mean metallicity of  $-0.5 \pm 0.2$  dex relative to the Sun, although their spectra do not sample the iron-group.

The stars in NGC 6822 are interesting themselves as well. Studies of very low-metallicity, massive stars need to be done in the dwarf irregular galaxies (the SMC being the most familiar) since extinction within the Galactic plane makes it too difficult to find and study any more nearby metal-poor young, massive stars in the outskirts of the Galaxy. Metallicity is recognized as a fundamental parameter in stars that affects star formation, stellar evolution, and stellar wind parameters. Thus, spectral analyses of stars in dwarf irregular galaxies offer a unique opportunity;

in particular, the results can be compared to the wealth of information published on stars in the Galaxy and Magellanic Clouds.

## 2. Observations and Reductions

Two A-type supergiants were initially selected from the literature (van den Bergh & Humphreys 1979); coordinates and color information are listed in Table 1. One of us (DJL) obtained low resolution spectra using EFOSC on the ESO 3.6m telescope on 17 September 1996, as part of a program to determine accurate spectral types for the brightest stars in Local Group galaxies. EFOSC was used in long-slit mode, with a 1.5" slit aligned on both stars. The B150 grism gave a resolution of  $\sim 8 \text{ \AA}$  and wavelength coverage from 3780 to 5510  $\text{\AA}$ . A single 30 minute exposure yielded S/N between 30 and 50, depending on wavelength. These observations confirmed that both stars are early A-type supergiants in NGC 6822, and thus they became our top priority for follow-up high resolution observations.

Observations of Star cc and Star m were made at Keck using HIRES (Vogt *et al.* 1994) on 26 & 27 September 1997 and 6 & 7 October 1999, respectively. Both stars received three one-hour exposures, and an extra half-hour exposure was made for Star cc. All observations were made through less than optimal conditions, including high humidity for Star cc and thin cirrus for Star m. For Star cc, seeing ranged from 1.0" to 1.3", thus a 1.1" slit was used, yielding resolving power of  $R=35,000$  over a 4 pixel resolution element. For Star m, subarcsecond seeing permitted a 0.86" slit, and thus slightly higher resolving power ( $R=45,000$ ). The spectra span  $4300 \leq \lambda \leq 6700 \text{ \AA}$  in 30 echelle orders, although the wavelength coverage is incomplete beyond  $\lambda 5200$  on the TK2048 CCD used. Slit length was limited to 7.0" to prevent overlapping orders at the short wavelength extreme. The two-dimensional CCD echelle spectrograms were reduced by JKM using the Figaro package, and a set of routines written specifically for echelle data reduction (c.f. McCarthy *et al.* 1995, McCarthy & Nemec 1997). Contamination by night sky lines and emission nebulae were removed from the stellar spectra prior to extraction by fitting low-order polynomials to "sky aperatures" adjacent to the stellar spectrum. Following optimal extraction (with cosmic ray removal), each echelle order was rebinned from 2048 to 1024 channels to increase the S/N per channel. The signal-to-noise in the rebinned and coadded HIRES spectra for Star cc is  $S/N = 35\text{-}56$  per 2-channel resolution element. The HIRES S/N for Star m was lower,  $S/N = 21\text{-}45$  per 2-channel resolution element. In both cases, the S/N improves in redder orders and decreases away from the center of each order.

An improved spectrum of Star m was obtained by AK with three two-hour exposures using UVES (D'Odorico & Kaper 2000) at the VLT on three consecutive nights, 8-10 October 1999, as part of the first UVES commissioning run at the second unit telescope UT2 ("Kueyen"). The spectrograph was set up in a predefined standard dichroic mode (Dichroic #1) with the blue central wavelength on cross-disperser #2 set to 390 nm and the red cross-disperser #3 to 564 nm, which gives nearly full wavelength coverage from  $<3600$  to 6657  $\text{\AA}$  (missing small blocks from

only 5610-5700 Å due to the dichroic mirror, and 4524-4637 Å due to the gap in between the red CCD mosaic). The three detectors in the two arms were used without binning and in low gain giving a read-out noise of  $< 4$  electrons. The seeing conditions varied from 0.5" to 0.9" over the three exposures, with an average seeing of 0.7". The spectrograph slit was set to a width of 1.0". Star m is located in a crowded field with nearby faint companions ( $\sim 2$ -5" separations). The field was derotated and the slit kept fixed at a constant position angle of 90 degrees. This further required the use of the atmospheric dispersion compensator (ADC) to optimize the slit throughput over the large wavelength range in the dichroic setting. The raw spectra are publically available through the ESO archive and were reduced with the ESO-MIDAS reduction package using the new UVES context (which is also the basis of the fully automatic data-reduction pipeline running at the telescope). For Star m, an optimum extraction algorithm with simultaneous cosmic ray rejection and sky-background subtraction was used. The three single flat-fielded and wavelength calibrated spectra from each spectrograph arm were then simply averaged with weights according to their S/N. The resultant spectra have resolution  $R=30,000$  over a 3 pixel resolution element. A signal-to-noise ratio of  $S/N = 50$ -70 per resolution element, was attained after coaddition.

Table 2 lists our identifications and equivalent width measurements for most of the stellar absorption lines in the spectra of these two stars. Very strong and/or blended lines have been neglected (though some strong lines are noted in italics, and some blended lines noted by "b", in cases where the line is listed because it is used in the other star). Figure 1 shows a comparison of equivalent width measurements for 33 lines in common between the UVES and the HIRES spectra for Star m. No significant offsets are apparent, and given the differences in the exposure times, S/N, and different observing conditions (e.g., weather, difference in airmass to NGC 6822), then we verify that the two instruments yield comparable spectra. The overall quality of our UVES spectrum of Star m is better (S/N and wavelength coverage), thus our analysis of Star m throughout this paper, and the equivalent widths listed in Table 2, are entirely from the UVES spectrum. Given the range in the S/N of the final spectra, the equivalent widths in Table 2 have an estimated uncertainty of  $\sim 10\%$  (highest S/N) to  $\sim 20\%$ .

### 3. Atmospheric Analyses

Both stars have been analysed using ATLAS9 (hydrostatic, line-blanketed, plane parallel) model atmospheres (Kurucz 1979, 1988). These atmospheres have been used successfully for photospheric analyses of A-F supergiants in the Galaxy, the Magellanic Clouds, and M31 (Venn *et al.* 2000, Venn 1999, 1995a, 1995b, Luck *et al.* 1998, Hill 1999, 1997, Hill *et al.* 1995).

Analyses of A-type supergiants requires a tailored analysis, where only weak spectral lines (preferably that form deep in the photosphere) are included. Weak lines are defined as lines where a change in microturbulence ( $\xi$ , discussed further below),  $\Delta\xi = \pm 1 \text{ km s}^{-1}$  yields a change in abundance of  $\log(X/H) \leq \pm 0.15$ . Typically,  $W_\lambda \leq 200 \text{ m}\text{\AA}$ . Using weak lines exclusively helps us to avoid uncertainties in the model atmospheres analysis due to neglected non-LTE and

spherical extension effects in the atmospheric structure, as well as non-LTE and  $\xi$  effects in the line formation calculations.

The critical spectral features used to determine the model atmosphere parameters (effective temperature,  $T_{\text{eff}}$ , and gravity) are the wings of the  $\text{H}\gamma$  line (e.g., see Figure 2) and ionization equilibrium of Mg I and Mg II (e.g., see Figure 3).  $\text{H}\gamma$  does not appear to be affected by a stellar wind component in either star; in fact, examination of  $\text{H}\alpha$  in both stars (see Figure 4) shows that neither has a strong wind (although some wind signatures can still be seen in both stars). A locus of  $T_{\text{eff}}$ -gravity pairs that reproduce the observed  $\text{H}\gamma$  profile and another locus where Mg ionization equilibrium occurs were examined, and their intersection point adopted for the best atmospheric parameters per star (e.g., see Figure 5).

Non-LTE calculations are included for Mg using the model atom developed by Gigas (1988) and a system of programs first developed by W. Steenbock at Kiel University and further developed and upgraded by M. Lemke. Mg non-LTE calculations in Galactic A-F supergiants have been described by Venn (1995b) for all but the lines near 3850 Å. The non-LTE corrections for all Mg lines used in this analysis are typically small ( $\leq 0.23$  dex), but including the corrections improves the atmospheric parameter determinations. For the two stars analysed here, the Mg non-LTE corrections are shown line by line in Table 3.

Comparing the two ionization states of iron cannot currently be used as a reliable atmospheric parameter indicator due to Fe I non-LTE effects, which are more complicated to model than Mg. Estimates of the  $\log(\text{Fe I}/\text{H})$  non-LTE corrections range from  $-0.2$  to  $\geq -0.3$  dex (c.f., Boyarchuk *et al.* 1985, Gigas 1986). However, non-LTE effects are expected to be negligible for Fe II lines, the dominant species of iron, as confirmed from detailed calculations by Becker (1998).

The microturbulence was found by examining the line abundances of Fe II and Cr II, and requiring no relationship with equivalent width. Examination of the Ti II lines suggested a lower microturbulence ( $\sim -1$  to  $-2$  km s $^{-1}$ ) for this species. Considering the weak lines nature of this analysis, and the estimated uncertainty of  $\Delta\xi = \pm 1$  km s $^{-1}$ , a single value for  $\xi$  was adopted for each star throughout.

The atmospheric parameters determined for both stars are listed in Table 1. Based on these parameters, new spectral types are assigned (by comparison to Galactic A supergiants with similar atmospheric parameters, see Venn 1995a). Uncertainties in  $T_{\text{eff}}$  are estimated from the range where  $\log(\text{Mg II}) = \log(\text{Mg I}) \pm 0.2$  when holding gravity fixed. This range allows for uncertainties in equivalent width measurements, atomic data, and uncertainties in the non-LTE calculations. Similarly, uncertainties in gravity are estimated from the range in the  $\text{H}\gamma$  profile fits while holding  $T_{\text{eff}}$  fixed (e.g., see Figure 2).

Intrinsic  $(\text{B}-\text{V})_o$  colors and bolometric corrections for each star are also determined from the

ATLAS9 model atmospheres using the Kurucz program UBVBUSER<sup>7</sup>. For Star cc and Star m,  $(B-V)_o = +0.05$  and  $+0.02$ , and  $B.C. = -0.15$  and  $-0.24$ , respectively. Comparing to the observed colors (Wilson 1992 photometry), colors have been dereddened using  $R_v = 3.1$ ; also the intrinsic luminosity ( $L/L_\odot$ ) has been determined after adopting the distance modulus ( $23.49 \pm 0.08$ ) from Gallart *et al.* (1996a). Luminosity and reddening are listed in Table 1, along with the radii determined from  $L/L_\odot$  and  $T_{\text{eff}}$ .

#### 4. Abundances

Elemental abundances were calculated using both spectrum synthesis and individual line width analyses. All calculations were done using a modified and updated version of LINFOR<sup>8</sup>.

In Table 2, the atomic data adopted from the literature are listed. An attempt was made to adopt laboratory measurements (e.g., O’Brien *et al.* 1991 for Fe I) and opacity project data (e.g., Biémont *et al.* (1991) for O I). Critically examined data were selected next (e.g., NIST data from Fuhr, Martin, & Wiese 1988 for Fe II), followed by the semi-empirical values calculated by Kurucz (1988). Solar abundances are from Grevesse & Sauval (1998).

Averaged elemental abundances per star are listed in Table 4 and plotted in Figure 6. Two error estimates are noted; the first is the line-to-line scatter ( $\sigma$ ), and the second is a *estimated* systematic uncertainty based on uncertainties in the atmospheric parameters. Abundance uncertainties due to model atmosphere parameters are shown in Table 5. The systematic uncertainty is probably an overestimate since we have simply added the possible uncertainties (in Table 5) in quadrature, not accounting for the fact that some  $T_{\text{eff}}$ -gravity combinations are excluded by the data (only for Mg I did we account for the excluded combinations). We also calculated the effect of the metallicity in the model atmosphere calculation by scaling the opacity distribution function by  $-0.4$  dex overall (or  $Z_\odot/3$ ), but found this affected the elemental abundances by  $\leq 0.03$  dex.

Oxygen abundances are primarily from the spectrum synthesis of the O I feature near 6158 Å; the spectra and LTE fits for both stars are shown in Figure 7. Synthesis of three Fe II lines ( $\lambda\lambda 6147, 6149, \text{ and } 6150 \text{ \AA}$ ) were done simultaneously with the O I synthesis. Results for rotational velocities, radial velocities, and macroturbulence were determined at this time and compared to spectrum syntheses of the magnesium and iron lines near 5200 Å and 4390 Å. The synthesis parameters are listed in Table 1. Abundances per line from the spectrum synthesis are listed in Table 2, and averaged for the best LTE oxygen abundance. Non-LTE corrections for oxygen are taken from the detailed calculations by Przybilla *et al.* (2000); based on the model atmosphere

---

<sup>7</sup>Program available from R. L. Kurucz at <http://cfaku5.harvard.edu/programs.html>

<sup>8</sup>LINFOR was originally developed by H. Holweger, W. Steffan, and W. Steenbock at Kiel University. It has been upgraded and maintained by M. Lemke, with additional modifications by N. Przybilla.

parameters, the corrections are  $-0.2$  and  $-0.3$  dex for Star cc and Star m, respectively. The final non-LTE oxygen abundances are listed in Table 4.

*Iron-group:* The Fe II results dominate our understanding of the metallicities in these two stars. This is because there are many spectral lines analysed which are relatively insensitive to uncertainties in the atmospheric parameters (other than  $\xi$ , but that is *determined* from Fe II itself), and not expected to suffer significant non-LTE effects. Cr II underabundances are in remarkably good agreement with those of Fe II in both stars. The Ni II abundance in Star m is slightly more underabundant than Fe II, but only two lines are sampled and the result is within the  $1\sigma$  errors. The difference of 0.2 dex in the Fe II abundance between Star m and Star cc is interesting (discussed further in Section 5.1), but could simply reflect the uncertainties in the analyses.

*Oxygen and the  $\alpha$ -elements:* The oxygen abundances in both stars were determined from a combination of spectrum synthesis and line analysis. For Star m, the spectrum synthesis favors a value near  $12+\log(\text{O}/\text{H})=8.5 \pm 0.1$  (LTE) for the blended 6155-6156 Å lines, yet synthesis and line analysis of the 6158 Å line favors an abundance of  $8.7 \pm 0.1$  (in LTE). We attribute this difference to the local S/N, since the lines are from the same multiplet (and have good atomic data which has been used to successfully determine the same line abundances of oxygen in Galactic stars in the past). An average LTE abundance is  $12+\log(\text{O}/\text{H})=8.58 \pm 0.17$  ( $\pm 0.09$ ) (where the different abundances for the 6158 Å line in Table 2 are themselves averaged a priori). The spectrum synthesis of oxygen for Star cc is more problematic. The synthesis parameters that best fit the two iron lines near 6148 Å (and checked with magnesium line fits in the blue) do not produce a spectrum that fits the O I 6158 line well. Thus, there is a significant disparity between the line abundance from its equivalent width and that from spectrum synthesis. We expect these difficulties arise from the S/N of the data at this feature. An average LTE abundance from the line abundances in Table 2 is  $12+\log(\text{O}/\text{H})=8.64 \pm 0.09$  ( $\pm 0.12$ ). The final abundances listed in Table 4 include the non-LTE corrections (discussed above).

Si II appears to be slightly more underabundant than the Mg abundances in these stars, although the same effect was seen in Galactic A-type supergiants. The Ti II underabundance is similar to O and Fe in Star cc, but it is  $\sim 0.2$  dex lower than Fe in Star m (this is similar to the Ni II result, yet it is determined from many more lines than Ni). A simple adjustment of the atmospheric parameters can bring the Ti result into better agreement with Fe, e.g.,  $\Delta\xi = -1 \text{ km s}^{-1}$ . Another possibility is a neglected Ti II non-LTE effect, a preliminary non-LTE syntheses of Ti II lines in A-supergiants (Becker 1998) suggests that the LTE abundances could be underestimated, as we have found. Sc II abundances are from very few lines, and we have neglected the hyperfine structure terms in this analysis, thus we shall not discuss those abundances further.

*s-process:* Only one line of Sr II is clearly detected and analysed in Star m ( $\lambda 4077.7$ ). Its underabundance is much greater than that of Fe II ( $[\text{Sr}/\text{Fe}] = -0.64 \pm 0.00$  ( $\pm 0.25$ ), which is not surprising considering the large underabundances of Sr found in the Galactic and SMC A-type

supergiants ( $[\text{Sr}/\text{Fe}] \sim -0.4$  and  $-1.0$ , respectively). Non-LTE probably affects the absolute Sr abundances, thus differential abundances should be more accurate. We find the differential Sr abundances, i.e.,  $\text{Sr}(\text{Star m}) - \text{Sr}(\text{SMC})$ , to be similar to the differential results for other elements.

## 5. Discussion

### 5.1. Present-day Chemistry of NGC 6822

For the first time, the present-day iron-group abundances have been determined from stars in NGC 6822. The mean underabundance is  $[\text{Fe}/\text{H}] = -0.49 \pm 0.22$  ( $\pm 0.21$ ). This is from the Fe II abundances, which are well supported by the results from the other iron-group elements, especially Cr II, where the mean  $[\text{Cr}/\text{H}] = -0.50 \pm 0.20$  ( $\pm 0.16$ ). In Table 6, all elemental abundances determined here are compared to solar, and differentially to the results from similar Galactic A-type supergiants (Venn 1995a,b) and SMC A-type supergiants (Venn 1999). A comparison of the differential results, confirms that these two stars have a metallicity that is slightly higher than that in the SMC (also see Figure 6).

We also notice that the Fe II abundance in Star cc is nearly 0.2 dex higher than in Star m. A line-by-line differential abundance comparison (from Table 2) shows  $\Delta \log(\text{Fe}/\text{H}) = +0.18 \pm 0.08$ . It is difficult to gauge the significance of this difference at present; it is  $>2 \sigma$ , but also close to the estimated systematic errors for Fe II from the atmospheric analysis of each star ( $\sim \pm 0.15$ ).

The mean oxygen abundance determined from the two stars,  $12 + \log(\text{O}/\text{H}) = 8.36 \pm 0.19$  ( $\pm 0.21$ ), is consistent with the nebular results,  $8.25 \pm 0.07$  (Pagel *et al.* 1980, or  $8.14 \pm 0.08$  considering only the three H II regions where O III was detected). Also, the two stellar oxygen abundances (8.28 and 8.44) are well within the range of the seven H II region results (e.g.,  $12 + \log(\text{O}/\text{H}) = 8.11$  from association ‘‘Hodge 15’’ and 8.50 from ‘‘Hodge 13’’). In fact, we note that the two stars analysed here are located near the center of NGC 6822, where Pagel *et al.* report oxygen of  $8.44 \pm 0.25$ . That the oxygen abundance from the stars is consistent with that from the nebulae is not surprising. Similar results have been found from recent analyses of B-stars in Orion (c.f., Cunha & Lambert 1994), the Galactic oxygen gradient from B-stars (c.f., Rolleston *et al.* 2000, and references therein), and B-K supergiant analyses in the SMC (c.f., Venn 1999, and references therein), M31 (Venn *et al.* 2000), and M33 (McCarthy *et al.* 1995, Monteverde *et al.* 2000).

In Table 6, one can easily see that the mean oxygen abundance from these two stars in NGC 6822 is less than solar, less than the Galactic A-type supergiants (this is significant since the Sun appears to have a higher oxygen abundance than the nearby stars and nebulae, see Meyer *et al.* 1998), and more than in the SMC stars. Similarly, the oxygen and iron overabundances relative to the SMC stars are nearly identical. Notice also in this Table that the mean underabundance of oxygen is the same as the mean underabundance of the other  $\alpha$ -elements (Mg, Si), when examined

relative to the Galactic A-type supergiants. Other elements (Ne & Ar) examined by the nebular analyses show underabundances ranging from  $-0.2$  to  $-0.6$  (Pagel *et al.* 1980, Skillman *et al.* 1989b), thus less than solar but greater than (or similar) to SMC abundances, consistent with the stellar results. Finally, Sr in Star m is less than solar, but considering the differential abundances, then Sr appears to be significantly overabundant relative to the Galactic and SMC A-supergiants.

## 5.2. Chemical Evolution of NGC6822

It is well known that the O/Fe ratio is a key constraint for the chemical evolution model of a galaxy. This is because O is primarily synthesized in Type II supernovae, whereas most of the Fe comes from Type Ia supernovae; thus a burst of star formation temporarily increases the O/Fe ratio in the ISM as massive stars quickly enrich the local ISM in O, while lower mass stars slowly increase the amount of Fe (Wheeler, Sneden, & Truran 1989, Gilmore & Wyse 1991).

We find a mean ratio of  $[O/Fe]=+0.02 \pm 0.20$  ( $\pm 0.21$ ) for the two stars analysed here. As seen in Table 6, our mean [O/Fe] ratio is similar to that of the SMC A-type supergiants (also note that the SMC A-supergiant results are in very good agreement with abundances from F-K supergiants, B-stars, and H II regions, see the discussion on differential SMC abundances by Venn 1999). This O/Fe ratio is also similar to that found from stars in the LMC (see Hill 1997, 1999, Hill *et al.* 1995, Russell & Bessell 1989, Luck *et al.* 1998, and Luck & Lambert 1992). This O/Fe ratio may also be similar to that of the Galactic disk stars at  $[Fe/H]=-0.5$ ; Edvardsson *et al.* (1993) show that [O/Fe] ranges from  $\sim +0.1$  to  $+0.25$  in Galactic F-G disk dwarfs at  $[Fe/H]=-0.5$ , which is slightly higher than our ratio but within our error range.

Our other mean  $\alpha$ -elements-to-iron ratio is similar to both the SMC A-supergiant results and the Galactic F-G disk dwarfs. In Table 6, the mean  $\alpha(Mg,Si)/Fe = +0.13 \pm 0.20$  ( $\pm 0.26$ ), while the mean from the SMC A-supergiants is  $+0.03 \pm 0.20$ . For the Galactic F-G disk dwarfs, Edvardsson *et al.* (1993) show that  $[Mg,Ti/Fe]$  ranges from  $+0.1$  to  $+0.3$  at  $[Fe/H]=-0.5$  (though  $[Si/Fe]$  looks slightly flatter, ranging from  $+0.05$  to  $+0.2$ ). This range overlaps the SMC results, and our new NGC 6822 results.

Analytical chemical evolution models for the Magellanic Clouds have been published by Pagel & Tautvaišienė (1998). These models show the predicted abundance ratios over a range of iron abundances. Our [O/Fe] and [Fe/H] results suggest that their models may also be appropriate for NGC 6822, even though the star formation histories in the Clouds are somewhat different from that determined in NGC 6822 by Gallart *et al.* (1996b,c). For example, a comparison of Figure 12 in Gallart *et al.* (1996c) and the bursting model of Figure 2 in Pagel & Tautvaišienė (1998) suggests that both galaxies have undergone recent bursts of star formation after a hiatus at intermediate ages<sup>9</sup>. However, the strength and timing of the recent bursts, and the details of

---

<sup>9</sup>The star formation history of the SMC is currently controversial, particularly with respect to a hiatus in the star

star formation in the older populations, are quite different.

Finally, our  $[\text{Sr}/\text{Fe}]$  ratio in Star m is interesting since the s-process elements are thought to form primarily by thermal-pulsing in intermediate-mass AGB stars. Thus, Sr samples a unique mass range (from O and Fe), an asset when reconstructing the star formation history of the galaxy. This can also be seen by the differences in the predicted Sr/Fe ratios in the Pagel & Tautvaišienė (1998) models for the Magellanic Clouds. Our one Sr/Fe ratio,  $[\text{Sr}/\text{Fe}] = -0.64 \pm 0.00 (\pm 0.25)$ , suggests that Sr is slightly less underabundant than in the A-F supergiants in the SMC, consistent with the results from other elements.

It is possible to observe additional elements in A-F supergiants, e.g., C, N, & S with observations at wavelengths from 7000 to 9500 Å. Nitrogen abundances would be interesting considering the very low nebular N abundances in NGC 6822 (Pagel *et al.* 1980, Kobulnicky & Skillman 1998), however surface N in A-supergiants is very likely to be enhanced through mixing with interior gas.

### 5.3. Spatial Abundance Variations

The two stars analysed here are located near the center of NGC 6822, and have similar elemental abundances to each other. The two stars do not span a significant range in locations in NGC 6822 to examine spatial abundance variations on their own, therefore we have calculated the galactocentric distances of these stars to compare to nebular abundances.

To calculate the NGC 6822 galactocentric distances, we have adopted the H I dynamical center coordinates ( $19^h 42^m 06.7^s$  and  $-14^\circ 55' 22.0''$ , 1950), position angle ( $112^\circ$ ), and inclination angle (inner part,  $50.1^\circ$ ) from Brandenburg & Skillman (1998). Our distances and the oxygen abundances for our two stars, Pagel *et al.*'s H II regions, and two planetary nebulae from Richer & McCall (1995) are listed in Table 7. We include the results from the two bright planetary nebulae considering that Richer (1993) has shown that the bright planetary nebulae in the Magellanic Clouds yield identical mean oxygen abundances as the H II regions (also see the discussion in Richer & McCall 1995).

When all of the data are examined together, we find no evidence for an abundance gradient in NGC 6822 (see Figure 8a). Pagel *et al.* (1980) came to the same conclusion from examination of the H II region data alone, although they were not aware of the orientation of the disk of NGC 6822. However, when only the most reliable of the data for the present-day oxygen

---

formation rate at intermediate epochs. For example, the ages and metallicities of intermediate-aged clusters can be interpreted as supporting either a smooth star formation rate (e.g., Da Costa & Hatzidimitriou 1998), or a bursting star formation history with an intermediate-aged hiatus (Mighell *et al.* 1998). Most dynamical models of the SMC, as well as the interpretation of the O/Fe ratio in the SMC, do suggest some form of a bursting star formation history, most likely related to interactions with the LMC and Galaxy (c.f., review by van den Bergh 2000, Chapter 7).

abundance are examined, i.e., the stellar data and the three H II regions where O III  $\lambda$ 4363 was detected (thus better electron temperatures), then a trend does emerge. There is the signature of an oxygen gradient with a slope near  $-0.18$  dex/kpc (see Figure 8b).

At this time, we do not suggest that we have found an actual abundance gradient in NGC 6822; we simply report that a selective subset of the data is consistent with a trend. As seen in Figure 8a, the data are also consistent with no trend at all. New spectroscopy of stars at larger distances and/or the H II regions could address this question. (It may be worth noting that these three H II regions do span across the full extent of the northern half of NGC 6822). A significant abundance gradient in NGC 6822 would be surprising, particularly one that is  $\sim 3x$  larger than that seen in the Galaxy (c.f., Rolleston *et al.* 2000, Shaver *et al.* 1983). Several other dwarf irregular galaxies have abundances from multiple H II regions, and yet, with the exception of NGC 5253, there are no cases of significant internal chemical fluctuations or abundance gradients (see Kobulnicky & Skillman 1997 and references therein). The lack of abundance variations in dwarf irregular galaxies has been interpreted as evidence against in situ enrichment (e.g., the instantaneous recycling approximation used in galaxy chemical evolution models), and thus a counter example would be intriguing.

#### 5.4. Reddening and Cepheid Distances

Foreground reddening to NGC 6822 is significant because of its low galactic latitude ( $\sim -18.4^\circ$ ). From our model atmospheres, the intrinsic  $(B-V)_o$  colors for our two stars were determined, and the reddening found to be  $E(B-V)=+0.29$  and  $+0.38$  for Star cc and Star m, respectively (see Table 1). Variable reddening has been found by several authors across NGC 6822. For example, Massey *et al.* (1995) found a systematic spatial trend from  $E(B-V)=0.26$  near the eastern and western most edges, and up to 0.45 near the bar of recently formed stars; other values of the mean (foreground +internal) reddening have ranged from  $\sim 0.2$  (Gallart *et al.* 1996a, Kayser 1967, Hodge 1977) to  $\sim 0.45$  (Wilson 1992, van den Bergh & Humphreys 1979). The values found for the two stars in this paper fall within this range, and are in good agreement with Massey *et al.* 's results since Star cc (near the eastern most edge) has a lower reddening than Star m (centrally located along the star-forming bar).

We have examined the positions of the eight Cepheid variables studied by Gallart *et al.* (1996a), who found a mean reddening of  $E(B-V)=+0.24 \pm 0.03$  to derive a true distance modulus to NGC 6822 of  $(m - M)_o=23.49 \pm 0.08$ . Four Cepheid variables (V1, V2, V3, and V13) are within  $1'$  of our supergiant targets, but only one Cepheid is truly near one of our targets; V3 is located  $9''$  ( $\sim 50$  pc) from Star cc. Adopting the Star cc reddening value, we predict the reddening for V3 is  $\sim 0.05$  magnitudes higher than the Gallart *et al.* mean value, yielding a slightly smaller distance modulus (although this difference is certainly within Gallart *et al.* 's errors). More interesting is the Cepheid V2, which appears to be centrally located in the star-forming bar, and is only  $23''$  ( $\sim 0.2$  kpc) from Star cc and  $34''$  ( $\sim 0.3$  kpc) from Star m. If this star has the higher reddening

attributed to stars in the central star-forming region, and supported by our Star m reddening result, then its reddening could be underestimated by as much as 0.2 magnitudes and its distance overestimated by  $\sim 10\%$  (45 kpc).

As Gallart *et al.* (1996a) discuss, the large and variable reddening to NGC 6822 is one of the largest problems in determining its true distance. A combination of spectroscopic stellar reddening measurements and new photometric monitoring of the known Cepheids could provide an improved distance to NGC 6822.

## 6. Conclusions and Future Work

We have presented the first stellar abundances in NGC 6822, which include O, other  $\alpha$ -elements, and iron-group abundances (plus one s-process element). Comparison of the oxygen abundances to those from H II regions shows that the stellar abundances are in excellent agreement with the nebulae. This has allowed us to examine the present-day O/Fe ratio in NGC 6822 for the first time. We find the mean  $[O/Fe]=+0.02 \pm 0.20$  ( $\pm 0.21$ ) is more similar to that in the SMC, than in metal-poor Galactic stars. We have also used the oxygen data to search for spatial abundance variations. Calculating NGC 6822 galactocentric distances using disk parameters from H I 21 cm synthesis observations shows no oxygen gradient when all data are considered. However, when only a subset of the most reliable oxygen abundances is used, the data are also consistent with a gradient of slope  $-0.18$  dex/kpc.

We recommend additional stellar and nebular spectroscopic analyses of NGC 6822 in the future to address the following questions;

- (1) Is there an oxygen abundance gradient in this dwarf irregular galaxy?
- (2) Is there a range in the iron-group abundances?

Finally, similar analyses of stars in other Local Group dwarf irregular galaxies will give us new information on O/Fe ratios for a variety of metallicities, and thus their star formation histories. Understanding the most metal-poor dwarf irregulars may be relevant to studies of high- $z$  galaxies, which are likely to be similarly metal-poor, pre-merger galaxies.

KAV would like to acknowledge financial support from the National Science Foundation, CAREER grant AST-9984073, the Henry Luce Foundation through a Clare Boothe Luce Professorship award, and from Macalester College. Also, KAV would like to thank Lissa Miller and Denis Foo Kune for research assistance, Carme Gallart for providing the Cepheid positions, and the referee B. E. Reddy for several helpful comments that improved this manuscript. JKM would like to thank the staff of the W. M. Keck Observatory, and in particular observing assistants Terry Stickel and Wayne Wack for their efforts on the summit in support of the Keck HIRES observations. SJS acknowledges financial support from the PPARC. EDS acknowledges financial

support from a NASA LTSA grant, NAG5-9221.

## REFERENCES

- Aaronson, M., Mould, J., Cook, K.H., 1985, *ApJ*, 291, L41
- Armandroff, T.E., Massey, P., 1985, *ApJ*, 291, 685
- Azzopardi, M., Lequeux, J., Maeder, A., 1988, *A&A*, 189, 34
- Becker S.R., 1998, *Boulder-Munich Workshop II: Properties of Hot Luminous Stars*, ASP Conf. Series, Vol. 131, 135
- Biémont, E., Hibbert, A., Godefroid, M., Vaeck, N., Fawcett, B.C., 1991, *ApJ*, 375, 818
- Boyarchuk, A.A., Lyubimkov, L.S., Sakhbullin, N.A., 1985, *Astrophysics*, 22, 203
- Brandenburg, H.J., Skillman, E.D., 1998, *BAAS*, 193, 7011
- Cunha, K., Lambert, D.L., 1994, *ApJ*, 426, 170
- D’Odorico, S., Kaper, L., 2000, *UVES User Manual*, ESO VLT-MAN-ESO-13200-1825
- Da Costa, G.S., Hatzidimitriou, D., 1998, *AJ*, 115, 1934
- Dufour, R.J., Talent, D.L., 1980, *ApJ*, 235, 22
- Edvardsson, B., Andersen, J., Gustafsson, B., Lambert, D.L., Nissen, P.E., Tomkin, J., 1993, *A&A*, 275, 101
- Elias, J.H., Frogel, J.A., 1985, 289, 141
- Fuhr, J.R., Martin, G.A., Wiese, W.L., 1988, *J. Phys. Chem. Ref. Data*, 17, Suppl. 4
- Fuhr, J.R., Martin, G.A., Wiese, W.L., Younger, S.M., 1981, *J. Phys. Chem. Ref. Data*, 10, 305
- Fuhr, J.R., Wiese, W.L., 1998, *CRC Handbook of Chemistry & Physics*, 79th Edition, ed. D.R. Lide, CRC Press, Inc., Boca Raton
- Gallart, C., Aparicio, A., Vilchez, J.M. 1996a, *AJ*, 112, 1928
- Gallart, C., Aparicio, A., Bertelli, G., Chiosi, C., 1996b, *AJ*, 112, 1950
- Gallart, C., Aparicio, A., Bertelli, G., Chiosi, C., 1996c, *AJ*, 112, 2596
- Garnett D.R., Skillman, E.D., Dufour, R.J., Peimbert, M., Torres-Peimbert, S. Terlevich, R., Terlevich, E., Shields, G., 1995, *ApJ*, 443, 64
- Gigas, D., 1986, *A&A*, 165, 170
- Gigas, D., 1988, *A&A*, 192, 264
- Gilmore, G., Wyse, R.F.G., 1991, *ApJ*, 367, L55
- Grevesse, N., Sauval, A.J., 1998, *Sp. Sci. Rev.*, 85, 161
- Herrero, A., Lennon, D.J., Vilchez, J.M., Kudritzki, R.P., Humphreys, R.H., 1994, *A&A*, 287, 885

- Hibbert, A., Biémont, E., Godefroid, M., Vaeck, N., 1991, *J. Phys. B*, 24, 3943
- Hill, V., 1997, *A&A*, 324, 435
- Hill, V., Andrievsky, S., Spite, M., 1995 *A&A*, 293, 347
- Hill, V., 1999, *A&A*, 345, 430
- Hodge, P.W., 1977, *ApJS*, 33, 69
- Hodge, P.W., 1980, *ApJ*, 241, 125
- Kayser, S.E., 1967, *AJ*, 72, 134
- Kobulnicky, H.A., Skillman, E.D., 1998, *ApJ*, 497, 601
- Kobulnicky, H.A., Skillman, E.D., 1997, *ApJ*, 489, 636
- Kudritzki, R.P., Puls, J., Lennon, D.J., Venn, K.A., Reetz, J., Najarro, F., McCarthy, J.K., Herrero, A., 1999, *A&A*, 350, 970 (Gal WLR)
- Kurucz, R.L., 1988, *Transactions of the IAU*, Vol. XXB, M. McNally, Kluwer, Dordrecht, 168
- Kurucz, R.L., 1979, *ApJS*, 40, 1
- Luck, R.E., Lambert, D.L., 1992, *ApJS*, 79, 303
- Luck, R.E., Moffett, T.J., Barnes, T.G., Gieren, W.P., 1998, *AJ*, 115, 605
- Lyubimkov, L.S., Boyarchuk, A.A., 1982, *Astrophysics*, 18, 596
- Maeder, A., Meynet, G., 2000, *ARA&A*, in press
- Martin, G.A., Fuhr, J.R., Wiese, W.L., 1988, *J. Phys. Chem. Ref. Data*, 17, Suppl. 3
- Massey, P., Armandroff, T.E., Pyke, R., Patel, K., Wilson, C.D., 1995, *AJ*, 110, 2715
- Mateo M., 1998, *ARA&A*, 36, 435
- McCarthy, J.K., Nemec, J.M., 1997, *ApJ*, 482, 203
- McCarthy, J.K., Lennon, D.J., Venn, K.A., Kudritzki, R.P., Puls, J., Najarro, F., 1995, *ApJ*, 455, 135
- Meyer, D.M., Jura, M., Cardelli, J.A., 1998, *ApJ*, 493, 222
- Mighell, K.J., Sarajedini, A., French, R.S., 1998, *AJ*, 116, 2395
- Monteverde, M.I., Herrero, A., Lennon, D.J., Kudritzki, R.P., 2000, *ApJ*, submitted
- Muschielok, B., Kudritzki R.P., *et al.* , 1999, *A&A*, 352, L40
- O’Brian, T.R., Wickliffe, M.E., Lawler, J.E., Whaling, W., Brault, J.W., 1991, *J. Opt. Soc. Am.*, B8, 1185
- Pagel, B.E.J., 1997, *Nucleosynthesis and the Chemical Evolution of Galaxies*, CUP, Cambridge
- Pagel, B.E.J., Edmunds, M.G., Smith, G., 1980 *MNRAS*, 193, 219
- Pagel, B.E.J., Tautvaišienė, G., 1998, *MNRAS*, 299, 535

- Przybilla, N., Butler, K., Becker, S.R., Kudritzki, R.P., Venn, K.A., 2000, *A&A*, submitted
- Przybilla, N., 1997, Diplomarbeit, Ludwig Maximilians Universität, München
- Richer, M.G., 1993, *ApJ*, 415, 240
- Richer, M.G., McCall, M.L., 1995, *ApJ*, 445, 642
- Rolleston, W.R.J., Smartt, S.J., Dufton, P.L., Ryans, R.S.I., 2000, *A&A*, in press
- Russell, S.C., Bessell, M.S., 1989, *ApJS*, 70, 865
- Shaver, P.A., McGee, R.X., Newton, L.M., Danks, A.C., Pottasch, S.R., 1983, *MNRAS*, 204, 53
- Sigut, T.A.A., Landstreet, J.D., 1990, *MNRAS*, 247, 611
- Skillman, E.D., Kennicutt, R.C., Hodge, P.W., 1989a, *ApJ*, 347, 875
- Skillman, E.D., Terlevich, R., Melnick, J., 1989b, *ApJ*, 347, 883
- van den Bergh, S., 2000, *The Galaxies of the Local Group*, Cambridge University Press, Cambridge
- van den Bergh, S., Humphreys, R.M., 1979, *AJ*, 84, 604
- Venn, K.A., 1995a, *ApJ*, 449, 839
- Venn, K.A., 1995b, *ApJS*, 99, 659
- Venn, K.A., 1999, *ApJ*, 518, 405
- Venn, K.A., McCarthy, J.K., Lennon, D.J., Przybilla, N., Kudritzki, R.P., Lemke, M., 2000, *ApJ*, in press
- Vogt, S. *et al.* , 1994, *SPIE*, 2198, 362
- Wiese, W.L., Smith, M.W., Miles, B.M., 1969, *NSRDS-NBS* 22
- Wheeler, J.C., Sneden, C., Truran, J., 1989, *ARA&A*, 27, 279
- Wilson, C., 1992, *AJ*, 104, 1374
- Wilson, C., 1995, *AJ*, 109, 449

Table 1. Coordinates and Color Information for Stars in NGC 6822

	Star cc	Star m
Names	A13 CW185	A101 CW173
$\alpha$ (J2000) <sup>a</sup>	19 44 53.4	19 44 56.5
$\delta$ (J2000) <sup>a</sup>	–14 46 42	–14 46 14
Hodge OB# <sup>a</sup>	10	...
V <sup>a</sup>	17.36 $\pm$ 0.01	17.38 $\pm$ 0.03
(B-V) <sup>a</sup>	+0.34	+0.40
<i>OLD Sp. Ty.</i> <sup>b</sup>	<i>B8-A0 I</i>	<i>A0 I</i>
<i>OLD V</i> <sup>b</sup>	<i>16.97</i>	<i>17.04</i>
<i>OLD (B-V)</i> <sup>b</sup>	<i>+0.36</i>	<i>+0.20</i>
<i>OLD E(B-V)</i> <sup>b</sup>	<i>+0.36</i>	<i>+0.20</i>
NEW Sp. Ty.	A3 Ia	A2 Ia
$T_{\text{eff}}$ (K)	8500 $\pm$ 150	9000 $\pm$ 150
log g	1.1 $\pm$ 0.1	1.3 $\pm$ 0.1
E(B-V)	+0.29	+0.38
log(L/L <sub>⊙</sub> )	4.78	4.92
R/R <sub>⊙</sub>	113	119
$\xi$ (km s <sup>–1</sup> )	6 $\pm$ 1	6 $\pm$ 1
$v \sin i$ (km s <sup>–1</sup> )	28 $\pm$ 2	15 $\pm$ 1
RV (km s <sup>–1</sup> )	–55 $\pm$ 2	–65 $\pm$ 2

Note. — Names A# from Kayser 1967, CW# from Wilson 1992.

<sup>a</sup>Magnitudes and colors from Wilson 1992, (also, OB association #, originally identified by Hodge 1977); coordinates from erratum (Wilson 1995).

<sup>b</sup>Magnitudes and colors from van den Bergh & Humphreys 1979. Their reddening estimates adopt (B-V)<sub>o</sub>=0.0 for both stars.

Table 2. Line Strengths, Atomic Data and Abundances

Elem	RMT	$\lambda$ (Å)	$\chi$ (eV)	log gf	REF <sup>†</sup>	accy	Star cc	Log $\epsilon$ (cc) <sub>LTE</sub>	Star m	Log $\epsilon$ (m) <sub>LTE</sub>
800	10	6155.99	10.74	-0.67	op		S	8.6	S	8.5
800	10	6156.78	10.74	-0.45	op		S	8.6	S	8.5
800	10	6158.19	10.74	-0.31	op		61/S	8.62/8.8	66/S	8.77/8.7
1200	3	3829.36	2.71	-0.21	fw	B	...	...	31	6.85
1200	2	5172.68	2.71	-0.38	fw	B	95	7.09	40	7.07
1200	2	5183.60	2.72	-0.16	fw	B	125	7.08	61	7.08
1201	5	3848.21	8.86	-1.56	fw	C	...	...	33	7.26
1201	10	4390.57	10.00	-0.50	fw	D	71	7.31	60	7.19
1401	1	3853.66	6.86	-1.60	fw	E	...	...	133	7.20
1401	1	3862.59	6.86	-0.90	fw	D+	...	...	210	7.26
1401	3	4128.07	9.84	0.31	fw	C	...	...	114	6.81
1401	3	4130.89	9.84	0.46	fw	C	...	...	133	6.86
1401	5	5041.02	10.07	0.17	fw	D+	118	7.37	103	7.09
1401	4	5957.56	10.07	-0.35	fw	D	37	6.99	45	7.02
1401	4	5978.93	10.07	-0.06	fw	D	...	...	63	7.00
2101	15	4314.08	0.62	-0.05	k88		137	2.92	38	2.64
2101	15	4320.73	0.61	-0.21	k88		135	3.06	≤20	...
2201	72	3741.63	1.58	-0.11	mfw	D	...	...	72	3.77
2201	34	3900.56	1.13	-0.44	mfw	D	...	...	90	3.93
2201	34	3913.48	1.12	-0.53	mfw	D	...	...	98	4.08
2201	11	4012.40	0.57	-1.61	mfw	C	...	...	47	4.35
2201	105	4163.63	2.59	-0.40	mfw	D	...	...	48	4.44
2201	105	4171.92	2.60	-0.56	mfw	D	...	...	30	4.37
2201	41	4290.22	1.16	-1.12	mfw	D-	...	...	55	4.30
2201	20	4294.09	1.08	-1.11	mfw	D-	...	...	36	4.02
2201	41	4300.06	1.18	-0.77	mfw	D-	...	...	91	4.27
2201	41	4301.92	1.16	-1.16	mfw	D-	...	...	35	4.11
2201	41	4307.90	1.16	-1.29	mfw	D-	220	...	41	4.32
2201	41	4312.86	1.18	-1.16	mfw	D-	151	4.67	40	4.19
2201	41	4314.97	1.16	-1.13	mfw	D-	88	4.20	36	4.09
2201	19	4395.03	1.08	-0.66	fmw	D-	200	4.44	87	4.05
2201	51	4399.77	1.24	-1.27	fmw	D-	116	4.58	21	4.02
2201	19	4443.80	1.08	-0.70	fmw	D-	196	4.44	83	4.06
2201	19	4450.48	1.08	-1.45	mfw	D-	89	4.46	≤20	...
2201	31	4501.27	1.12	-0.75	mfw	D-	142	4.13	77	4.09
2201	50	4563.76	1.22	-0.96	mfw	D-	151	4.47	...	...
2201	82	4571.96	1.57	-0.52	mfw	D-	191	4.55	...	...
2201	92	4805.09	2.06	-1.12	fmw	D-	81	4.72	20	4.36
2201	114	4874.01	3.09	-0.79	mfw	D	46	4.77	≤20	...
2201	70	5154.07	1.57	-1.92	mfw	D-	52	4.91	≤20	...
2201	70	5226.54	1.57	-1.29	mfw	D-	136	4.90	b	...
2401	18-26	4111.00	3.74	-1.92	k88		...	...	39	5.43
2401	31	4242.36	3.87	-1.17	sl		...	...	53	4.92
2401	31	4261.91	3.87	-1.34	sl		...	...	56	5.12
2401	31	4275.57	3.86	-1.52	sl		...	...	47	5.19

Table 2—Continued

Elem	RMT	$\lambda$ (Å)	$\chi$ (eV)	log gf	REF <sup>†</sup>	accy	Star cc	Log $\epsilon$ (cc) <sub>LTE</sub>	Star m	Log $\epsilon$ (m) <sub>LTE</sub>
2401	31	4284.19	3.86	-1.67	sl		...	...	34	5.18
2401	44	4555.00	4.07	-1.30	sl		76	5.20	...	...
2401	44	4616.63	4.07	-1.36	sl		63	5.15	...	...
2401	44	4618.80	4.07	-0.84	sl		139	5.21	...	...
2401	44	4634.10	4.07	-0.99	sl		105	5.11	...	...
2401	30	4812.34	3.86	-1.96	sl		29	5.10	≤25	...
2401	30	4824.13	3.87	-0.97	sl		181	5.50	107	5.15
2401	30	4848.24	3.86	-1.15	sl		118	5.22	90	5.19
2401	30	4876.41	3.86	-1.46	sl		98	5.38	60	5.25
2401	43	5237.33	4.06	-1.16	mfw	D	89	5.14	66	5.13
2401	43	5274.96	4.05	-1.29	k88		64	5.06	56	5.16
2600	21	3787.88	1.01	-0.84	ob		...	...	21	7.35
2600	20	3820.43	0.86	0.16	ob		...	...	80	6.96
2600	20	3825.88	0.91	-0.03	ob		...	...	47	6.87
2600	4	3859.91	0.00	-0.71	fmw	B+	...	...	50	7.00
2600	43	4063.60	1.56	0.06	ob		...	...	29	6.93
2600	42	4325.76	1.61	0.01	ob		83	7.11	b	...
2600	41	4383.54	1.48	0.21	ob		104	6.97	b	...
2600	41	4404.75	1.56	-0.15	ob		59	7.03	≤20	...
2600	318	4891.50	2.85	-0.11	ob		31	7.50	≤20	...
2601	14	3783.35	2.27	-3.16	k88		...	...	110	6.95
2601	3	3945.21	1.70	-4.25	fmw	D	...	...	53	7.19
2601	28	4122.64	2.58	-3.38	fmw	D	...	...	50	6.82
2601	27	4173.45	2.58	-2.18	fmw	C	...	...	162	6.55
2601	28	4178.86	2.58	-2.48	fmw	C	...	...	170	6.91
2601	28	4258.15	2.70	-3.40	fmw	D	...	...	54	6.95
2601	27	4273.32	2.70	-3.34	fmw	D	...	...	48	6.82
2601	28	4296.57	2.70	-3.10	mfw	D	...	...	82	6.82
2601	27	4303.17	2.70	-2.49	fmw	D	...	...	176	7.04
2601	27	4351.77	2.70	-2.10	fmw	C	280	...	208	6.93
2601	27	4385.38	2.78	-2.57	fmw	D	188	7.08	123	6.74
2601	27	4416.83	2.78	-2.61	fmw	D	160	6.89	130	6.83
2601	37	4472.92	2.84	-3.43	fmw	D	96	7.28	55	7.07
2601	37	4489.18	2.83	-2.97	fmw	D	138	7.12	99	6.99
2601	37	4491.40	2.86	-2.69	fmw	C	155	6.99	110	6.81
2601	38	4508.29	2.86	-2.22	fmw	D	228	...	193	7.00
2601	37	4515.34	2.84	-2.48	fmw	D	230	...	160	6.97
2601	37	4520.22	2.81	-2.61	fmw	D	175	7.02	133	6.87
2601	38	4541.52	2.86	-3.05	fmw	D	91	6.87	...	...
2601	38	4576.34	2.84	-3.04	fmw	D	118	7.05	...	...
2601	37	4582.84	2.84	-3.09	fmw	C	102	6.98	...	...
2601	186	4635.32	5.96	-1.65	fmw	D-	66	7.21	...	...
2601	43	4656.98	2.89	-3.63	fmw	E	80	7.38	b	...
2601	37	4666.75	2.83	-3.33	fmw	D	90	7.12	64	7.05
2601	43	4731.45	2.89	-3.37	fmw	D	94	7.23	53	7.02

Table 2—Continued

Elem	RMT	$\lambda$ (Å)	$\chi$ (eV)	log gf	REF <sup>†</sup>	accy	Star cc	Log $\epsilon$ (cc) <sub>LTE</sub>	Star m	Log $\epsilon$ (m) <sub>LTE</sub>
2601	49	5197.57	3.23	-2.10	fmw	C	205	7.00	140	6.68
2601	49	5234.62	3.22	-2.05	fmw	C	222	...	167	6.83
2601	48	5264.81	3.23	-3.19	fmw	D	...	...	37	6.85
2601	185	5272.40	5.96	-2.03	fmw	D	...	...	33	7.26
2601	44	5276.00	3.20	-1.95	fmw	C	231	...	170	6.74
2601	41	5284.10	2.89	-3.19	fmw	D	106	7.13	56	6.87
2601	48	5362.86	3.20	-2.74	k88		148	7.19	91	6.92
2601	49	5425.25	3.20	-3.36	fmw	D	...	...	37	7.00
2601		5506.20	10.52	0.95	fmw	D	...	...	32	6.88
2601	55	5534.85	3.24	-2.92	fmw	D	...	...	77	7.01
2601	74	6147.74	3.89	-2.46	fmwy*	D	91	6.97	68	6.89
2601	74	6149.24	3.89	-2.77	fmw*	D	100	7.35	60	7.12
2601	74	6238.38	3.89	-2.48	k88		89	6.97	40	6.61
2601	74	6247.56	3.89	-2.36	fmw*	D	140	7.24	105	7.11
2601	74	6416.91	3.89	-2.70	fmw*	D	...	...	60	7.06
2801	11	3849.55	4.01	-1.88	k88		...	...	46	5.45
2801	11	4067.03	4.03	-1.84	k88		...	...	56	5.54
3801	1	4077.71	0.00	0.15	k88		...	...	14	1.71

<sup>†</sup>Reference Key: fw = Fuhr & Wiese 1998, fmw = Fuhr *et al.* 1988, fmwy = Fuhr *et al.* 1981, k88 = Kurucz 1988 (CD-18), mfw = Martin *et al.* 1988, ob = O'Brien *et al.* 1991, op = Hibbert *et al.* 1991, sl = Sigut & Landstreet 1990, wsm = Wiese, Smith, & Miles 1969. Some FeII adjusted for the lower solar FeII abundance than used in the original reference (loggf-0.15 denoted by \*). Capital letters denote estimated accuracy (where uncertainties of gf values are within 3%=A, 10%=B, 25%=C, 50%=D).

Table 3. Magnesium Line NLTE corrections

$\lambda$ (Å)	Levels	$\chi$ (eV)	$\log(gf)$	REF	Star cc			Star m		
					EQW	LTE	NLTE	EQW	LTE	NLTE
Mg I										
3829.36	$3p^3P^0 - 3d^3D$	2.71	-0.21	fwB		...		31	6.85	7.08
5172.68	$3p^3P^0 - 4s^3S$	2.71	-0.38	fwB	95	7.11	7.31	40	7.07	7.30
5183.60	$3p^3P^0 - 4s^3S$	2.71	-0.16	fwB	125	7.10	7.29	60	7.07	7.30
Mg II										
3848.21	$3d^2D - 5p^2P^0$	8.86	-1.56*	fwC		...		33	7.26	7.31
4390.57	$4p^2P^0 - 5d^2D$	10.00	-0.50*	fwD	71	7.31	7.34	60	7.20	7.21

Note. — The magnesium NLTE corrections have been computed using the model atom by Gigas 1988. Reference for the atomic data are from Fuhr & Wiese 1998 (with estimated accuracies noted in capitals).

\*These lines are a clean blend of two to three lines from the same multiplet. Their gf-values have been added together since the wavelengths are nearly identical

Table 4. Elemental Abundances  $\pm\sigma$  (# lines)  $\pm$ systematic

Elem	Solar	Star cc	Star m
O I NLTE <sup>a</sup>	8.83	8.44 $\pm$ 0.09 ( 3) $\pm$ 0.12	8.28 $\pm$ 0.17 ( 3) $\pm$ 0.09
Mg I NLTE <sup>a</sup>	7.58	7.30 $\pm$ 0.02 ( 2) $\pm$ 0.20 <sup>b</sup>	7.23 $\pm$ 0.13 ( 3) $\pm$ 0.20 <sup>b</sup>
Mg II NLTE <sup>a</sup>	7.58	7.34 $\pm$ 0.00 ( 1) $\pm$ 0.10	7.26 $\pm$ 0.06 ( 2) $\pm$ 0.06
Si II	7.56	7.18 $\pm$ 0.19 ( 2) $\pm$ 0.14	7.03 $\pm$ 0.17 ( 7) $\pm$ 0.18
Sc II	3.10	2.99 $\pm$ 0.09 ( 2) $\pm$ 0.30	2.64 $\pm$ 0.00 ( 1) $\pm$ 0.22
Ti II	4.94	4.55 $\pm$ 0.23 (13) $\pm$ 0.25	4.16 $\pm$ 0.16 (18) $\pm$ 0.15
Cr II	5.69	5.22 $\pm$ 0.13 (10) $\pm$ 0.14	5.17 $\pm$ 0.17 (10) $\pm$ 0.07
Fe I	7.50	7.15 $\pm$ 0.30 ( 4) $\pm$ 0.32	7.03 $\pm$ 0.24 ( 5) $\pm$ 0.23
Fe II	7.50	7.10 $\pm$ 0.15 (20) $\pm$ 0.17	6.92 $\pm$ 0.16 (35) $\pm$ 0.13
Ni II	6.25	...	5.49 $\pm$ 0.06 ( 2) $\pm$ 0.05
Sr II	2.93	...	1.71 $\pm$ 0.00 ( 1) $\pm$ 0.25

Note. — Two uncertainties are listed for each element per star. First is the line-to-line scatter in the abundances ( $\sigma$ ) followed by the number of lines in the average. Second is an estimate of the potential systematic errors due to uncertainties in the atmospheric parameters (see Table 5). This second uncertainty is noted in italics and it is probably an overestimate (adding in quadrature does not account for  $T_{\text{eff}}$ -gravity pairs that can be discounted).

<sup>a</sup>Oxygen NLTE corrections of  $-0.2$  and  $-0.3$  have been applied to Star cc and Star m, respectively, as determined by Przybilla *et al.* (2000). Magnesium NLTE corrections are discussed further in Table 3.

<sup>b</sup>The systematic uncertainty for Mg I has been set to  $\pm 0.20$  after considering only the allowed  $T_{\text{eff}}$ -gravity pairs.

Table 5. Abundance Uncertainties

Elem	$\Delta T = +150 \text{ K}$	$\Delta \log g = -0.1$	$\Delta \xi = -1 \text{ km s}^{-1}$
	Star cc / Star m	Star cc / Star m	Star cc / Star m
O I	0.08 / 0.06	0.08 / 0.05	0.04 / 0.04
Mg I	0.27 / 0.22	0.19 / 0.16	0.07 / 0.01
Mg II	0.03 / 0.03	0.07 / 0.05	0.06 / 0.02
Si II	-0.03 / -0.02	0.02 / -0.01	0.14 / 0.16
Sc II	0.24 / 0.20	0.13 / 0.08	0.13 / 0.01
Ti II	0.18 / 0.14	0.10 / 0.05	0.14 / 0.03
Cr II	0.09 / 0.06	0.05 / 0.01	0.09 / 0.04
Fe I	0.26 / 0.20	0.18 / 0.11	0.04 / 0.01
Fe II	0.08 / 0.05	0.04 / 0.01	0.15 / 0.12
Ni II	... / 0.01	... / -0.02	... / 0.04
Sr II	... / 0.23	... / 0.10	... / 0.01

Table 6. Differential Abundances

Elem	Solar	Gal AIs* –Solar	SMC* –Solar	Star cc –Solar	Star m –Solar	Mean(cc,m) –Solar	Mean(cc,m) –GAL AIs	Mean(cc,m) –SMC AIs
O I	8.83	–0.24	–0.69	–0.39	–0.55	–0.47	–0.23	+0.22
Mg I	7.58	–0.10	–0.76	–0.28	–0.35	–0.32	–0.22	+0.45
Mg II	7.58	–0.12	–0.75	–0.24	–0.32	–0.28	–0.16	+0.47
Si II	7.56	–0.22	–0.58	–0.38	–0.53	–0.46	–0.24	+0.13
Sc II	3.10	+0.04	–0.81	–0.11	–0.46	–0.29	–0.33	+0.52
Ti II	4.94	–0.07	–0.64	–0.39	–0.78	–0.59	–0.52	+0.08
Cr II	5.69	–0.07	–0.71	–0.47	–0.52	–0.50	–0.43	+0.21
Fe I	7.50	+0.05	–0.89	–0.35	–0.47	–0.41	–0.46	+0.48
Fe II	7.50	–0.11	–0.73	–0.40	–0.58	–0.49	–0.38	+0.24
Ni II	6.25	...	...	...	–0.76	–0.76 <sup>a</sup>	...	...
Sr II	2.93	–0.52	–1.72	...	–1.22	–1.22 <sup>a</sup>	–0.70 <sup>a</sup>	+0.50 <sup>a</sup>
O I/Fe II		–0.13	+0.04	+0.01	+0.03	+0.02	+0.15	–0.02
$\alpha(\text{Mg,Si})/\text{Fe II}$		–0.04	+0.03	+0.09	+0.16	+0.13	+0.17	+0.10
Sr II/Fe II		–0.41	–0.99	...	–0.64	–0.73 <sup>a</sup>	–0.32 <sup>a</sup>	+0.26 <sup>a</sup>

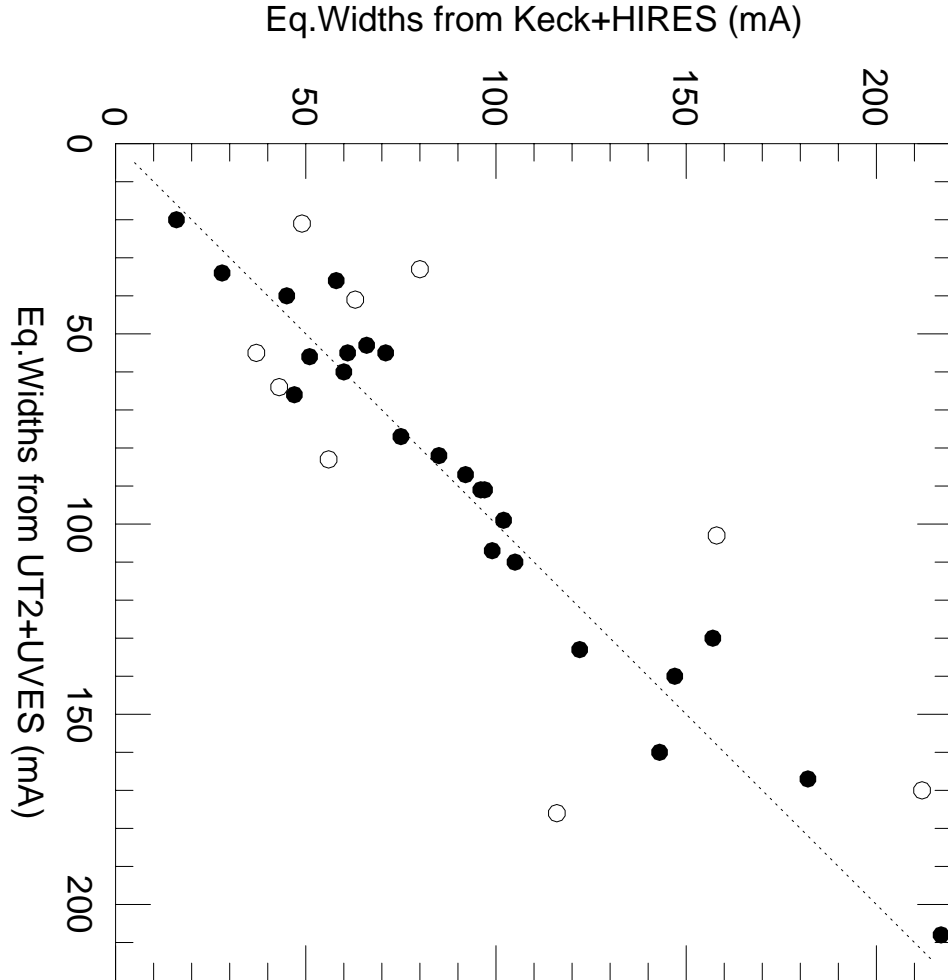
\*The Galactic and SMC A-supergiant abundances are those discussed in Table 6 of Venn 1999.

<sup>a</sup>“Mean” value is from only one star.

Table 7. Distances and Oxygen Abundances

Object	12+log(O/H)	D (kpc)
STARS		
Star m	8.28 ±0.17	0.28
Star cc	8.44 ±0.09	0.27
H II		
Ho 11	8.24 ±0.20	0.78
Ho 12	8.23 ±0.20	0.85
Ho 3*	8.21 ±0.15	0.77
Ho 6/8*	8.20 ±0.09	0.85
Ho 14	8.27 ±0.20	1.28
Ho 13	8.50 ±0.20	1.45
Ho 15*	8.11 ±0.12	1.59
Nucleus	8.44 ±0.25	0.06
PN		
S33	8.01 ±0.16	0.30
S16	8.10 ±0.08	0.49

Note. — Oxygen abundances for the H II regions from Pagel *et al.* (1980; a \* notes those with O III measurements), and for the planetary nebulae from Richer & McCall (1995). Distances are calculated using NGC 6822 H I dynamical center coordinates ( $19^h 42^m 06.7^s$ ,  $-14^\circ 55' 22.0''$ , 1950), position angle ( $122^\circ$ ), and inclination ( $50.1^\circ$ ) from Brandenburg & Skillman (1998).



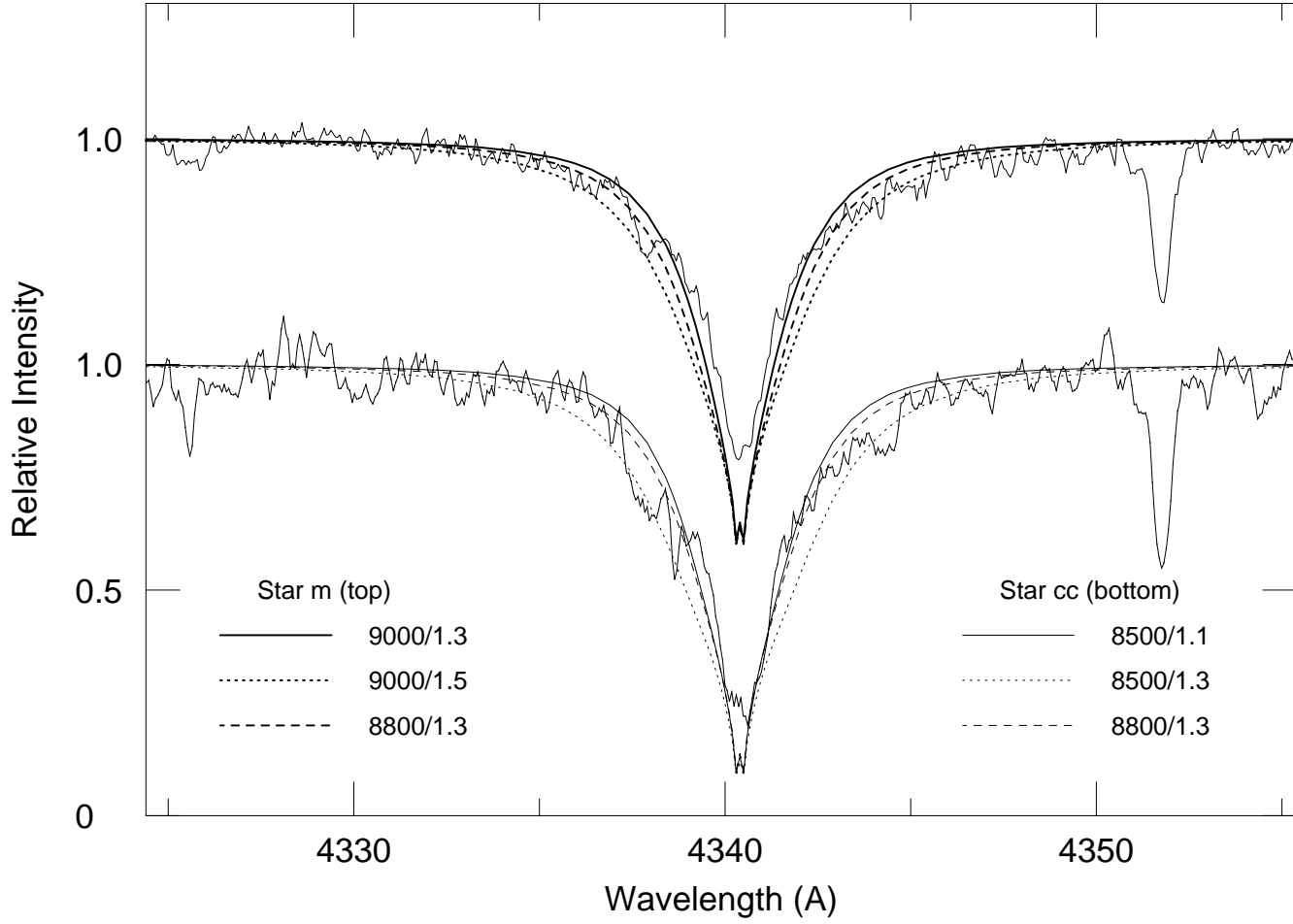


Fig. 2.—  $H\gamma$  profiles for Star m (top) and Star cc (bottom). Theoretical fits are shown for  $T_{\text{eff}}/\log g$  pairs for both stars.

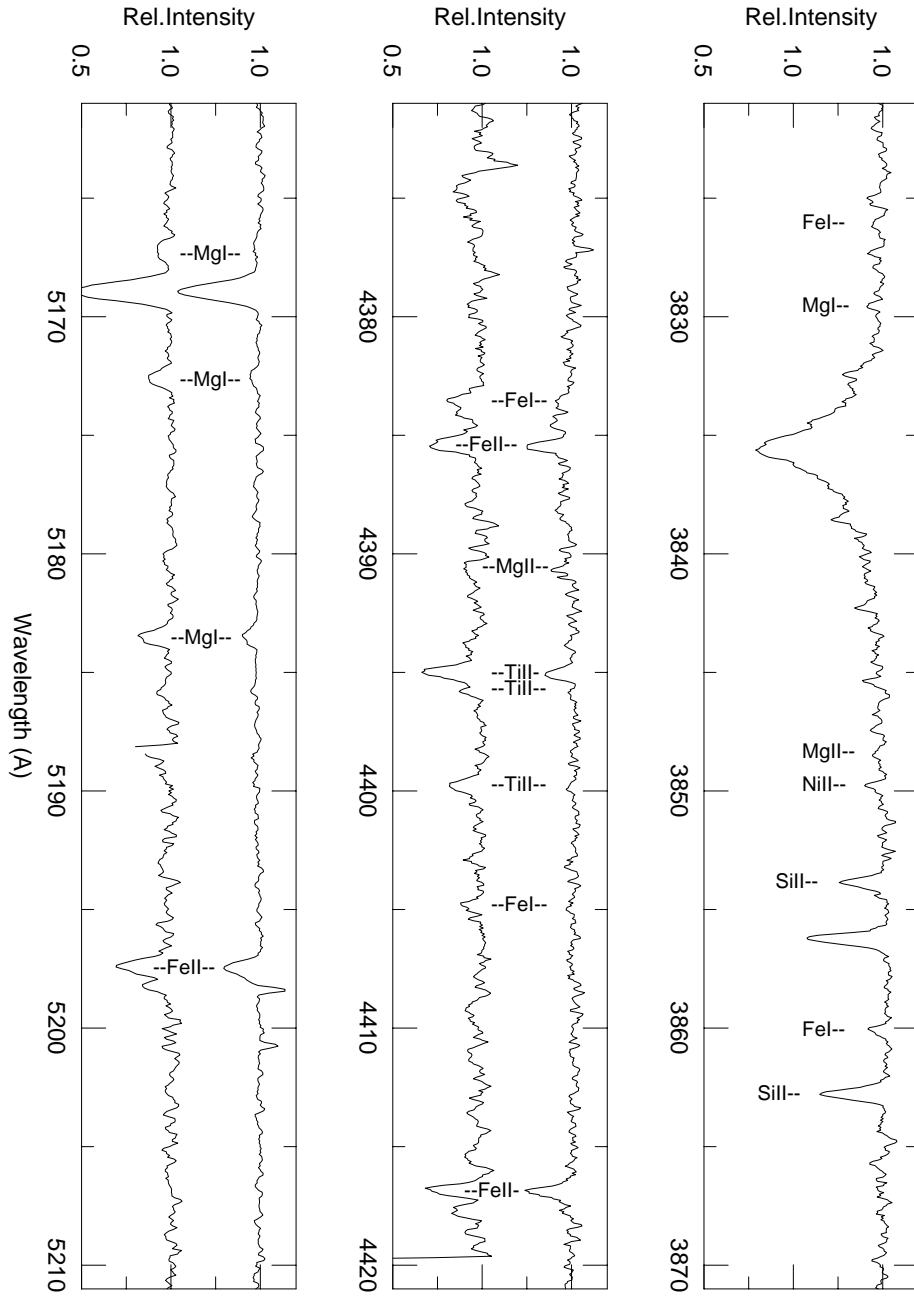


Fig. 3.— Sample spectra of Star m (top) and Star cc (bottom) around the critical Mg I and Mg II lines.

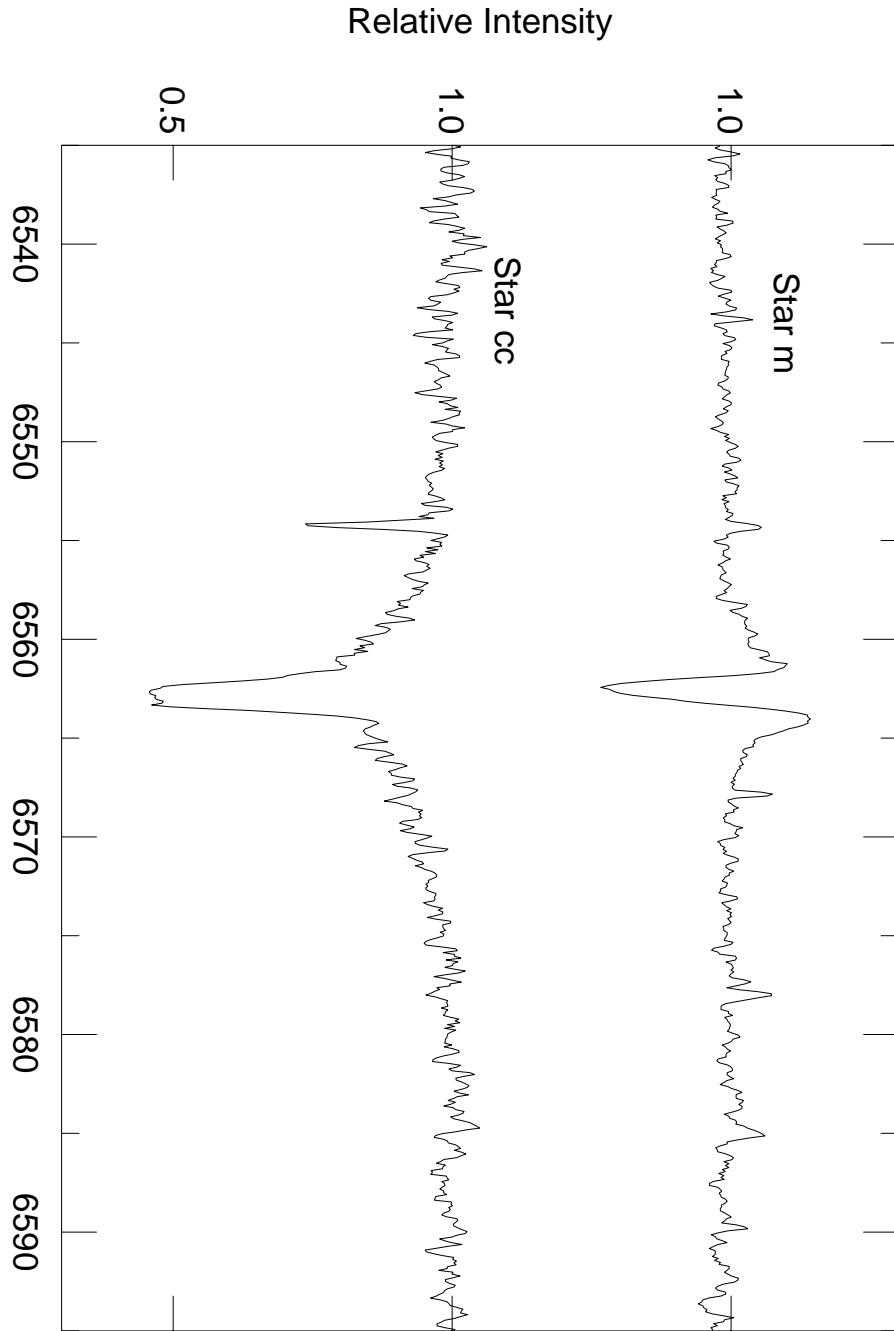


Fig. 4.—  $H\alpha$  spectra for Star m (top) and Star cc (bottom). Neither shows evidence of a strong stellar wind, such as a P Cygni profile.

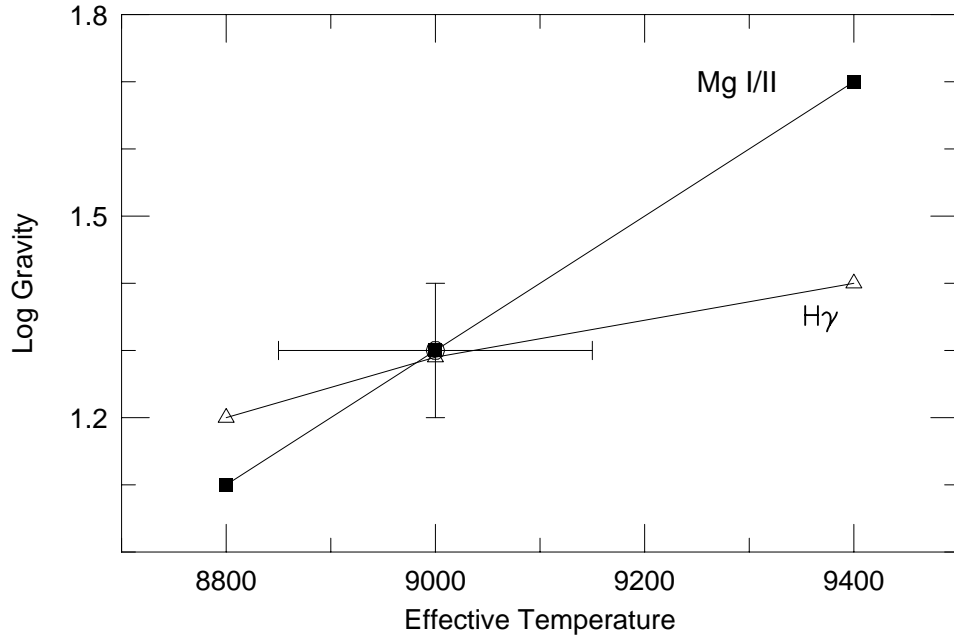


Fig. 5.—  $T_{\text{eff}}$ -gravity pairs that fit the spectral features of Star m. *Hollow triangles* track  $H\gamma$  fits; *filled squares* follow the Mg ionization equilibrium.

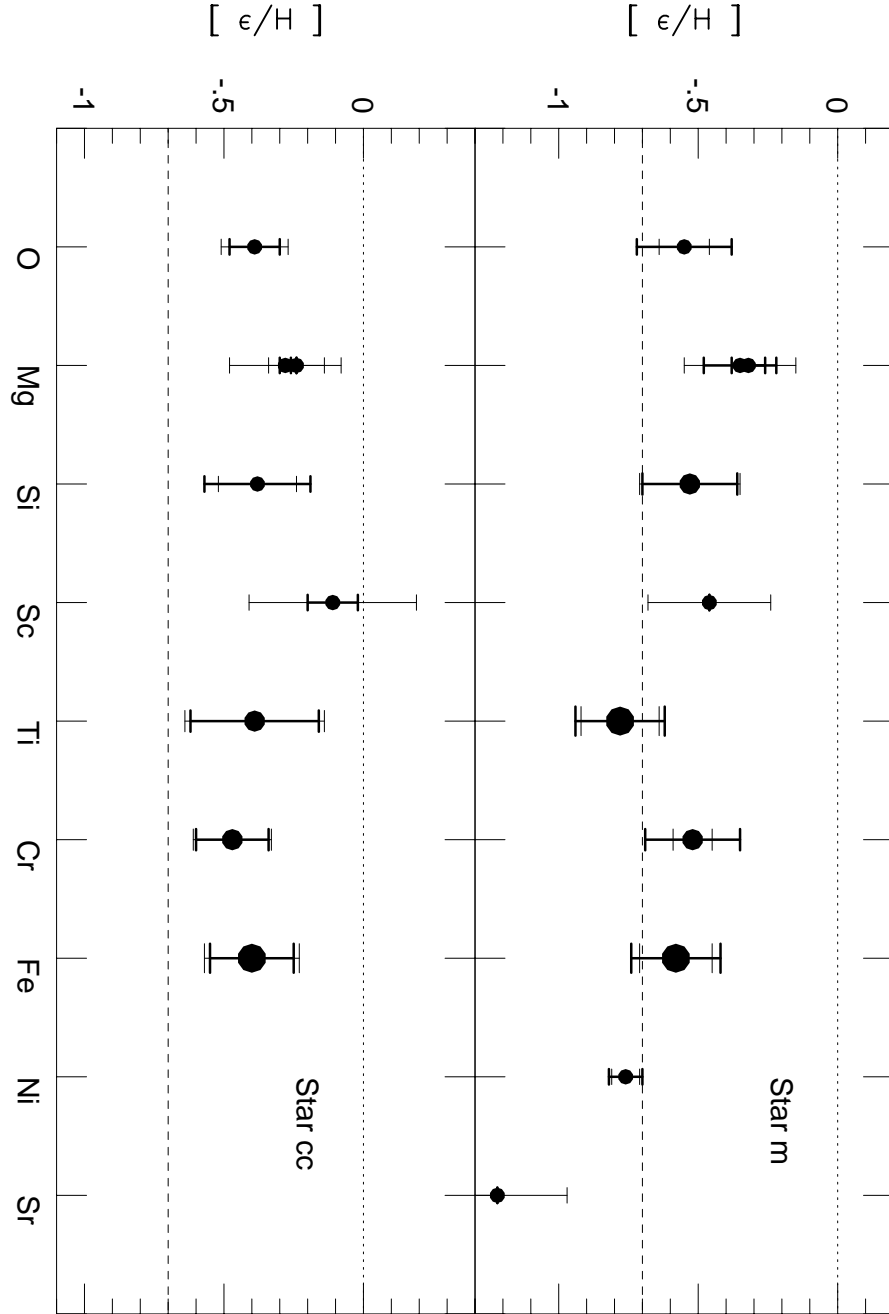


Fig. 6.— Elemental abundances for Star m (top) and Star cc (bottom) relative to the the Sun. Two errorbars are shown for each point; *thick line* for the line-to-line scatter, and *thin line* for the systematic uncertainties (see Table 4). The largest data points include  $\geq 16$  line abundances, and the smallest include  $\leq 5$ . The mean SMC underabundance is noted by the *dashed line* (although note that the SMC A-supergiant Sr result is off the dashed line and this graph at -1.7).

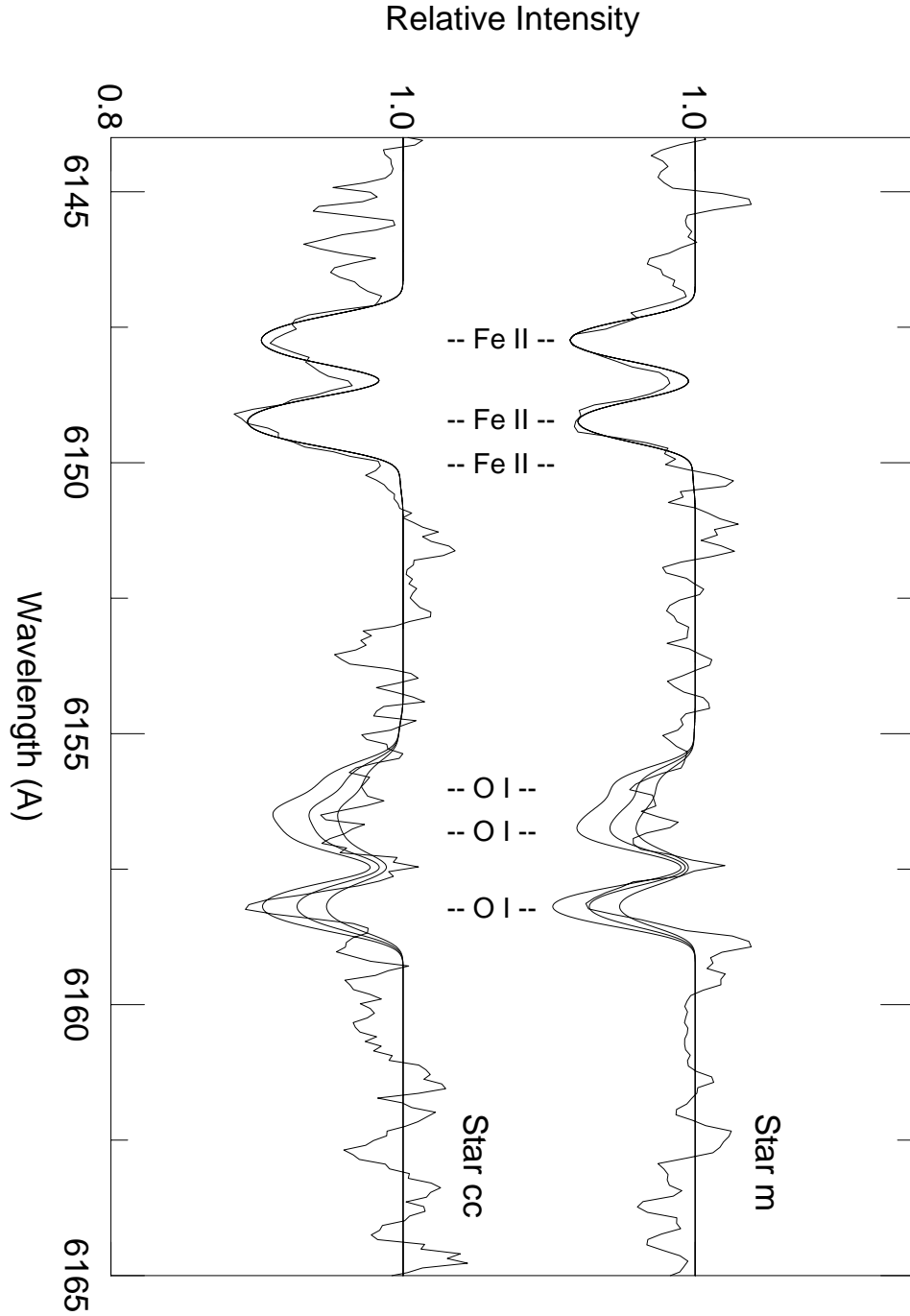


Fig. 7.— Spectrum synthesis of the O I  $\lambda$ 6155-6158 lines, as well as the Fe II lines near  $\lambda$ 6148, for Star m (top) and Star cc (bottom). Three oxygen abundances are shown,  $12+\log(\text{O}/\text{H})=8.5, 8.7, 8.9$ . The spectrum synthesis parameters are those listed in Table 1, and the iron line abundances are those listed in Table 2.

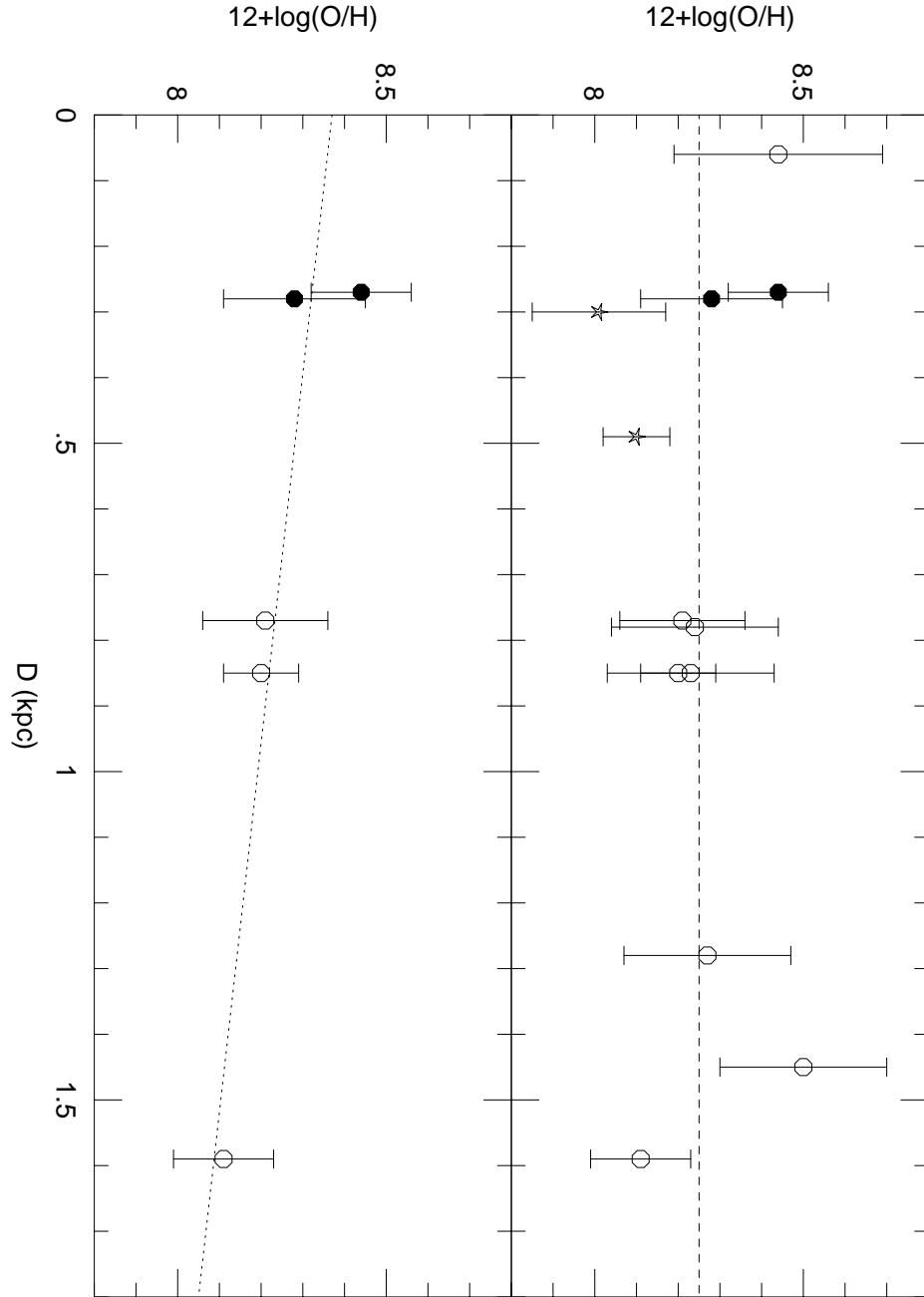


Fig. 8.— Oxygen abundances versus NGC 6822 galactocentric distance. *Filled circles* represent the stellar data, *hollow circles* show the Pagel *et al.* (1980) nebular data, and *hollow stars* note two planetary nebulae results from Richer & McCall (1995). The *dashed line* in the top panel shows the mean oxygen abundance from Pagel *et al.* ( $12+\log(\text{O}/\text{H})=8.25$ ). In the bottom panel, only the stellar abundances and those from H II regions where O III was detected are shown. A least squares fit to the data (*dotted line*) suggests a slope of  $-0.18$  dex/kpc.